Catalysis Today xxx (2015) xxx–xxx

Contents lists available at ScienceDirect

Catalysis Today

journal homepage: www.elsevier.com/locate/cattod

Total oxidation of naphthalene using copper manganese oxide catalysts

Tomos J. Clarke, Simon A. Kondrat, Stuart H. Taylor*

Cardiff Catalysis Institute, School of Chemistry, Cardiff University, Main Building, Park Place, Cardiff CF10 3AT, UK

ARTICLE INFO

Article history:
Available online xxx

Keywords:
Copper manganese oxide
Hopcalite
Catalytic oxidation
Naphthalene
Polyaromatic hydrocarbons
VOCs

ABSTRACT

A series of copper manganese oxide catalysts have been investigated for the total oxidation of naphthalene, selected as a model compound for oxidation of polyaromatic hydrocarbons. Catalysts were prepared by coprecipitation and were calcined at 300, 400, 500 and 600 °C. The catalyst most active and selective towards CO_2 was calcined at 400 °C, and this was related to the formation of a high surface area poorly crystalline $CuMn_2O_4$ phase. Catalysts calcined at 500 and 600 °C were less effective in oxidising naphthalene to CO_2, and their composition of more highly crystalline $CuMn_2O_4$, with Mn_2O_3 for the 600 °C catalyst, formed partial oxidation products. There was also a direct relationship between the extent of reduction from temperature programmed reduction and catalyst performance.

1. Introduction

Catalytic oxidation of volatile organic compounds (VOCs) is recognised as being a highly effective process for controlling their aerial emissions [1]. Whilst catalytic total oxidation of VOCs have been studied widely, some specific types of VOCs have received less attention. One such example is poly-aromatic hydrocarbons (PAHs), which are produced from a wide range of combustion processes and have been linked with serious health risks [2,3]. However, more recently, attention has started to focus on the catalytic total oxidation of PAHs [4]. Naphthalene has often been selected as a model PAH for study, as it is relatively less toxic to handle and its behaviour during catalytic oxidation can be extrapolated to more complex higher molecular weight PAHs.

In one of the earliest studies on naphthalene catalytic oxidation, Zhang et al. [5] used a series of metal catalysts supported on γ-Al_2O_3. The most effective were those containing platinum, and initial studies focused on precious metals, showing that they were generally more active than metal oxide catalysts [6,7]. The effect of support was also important and studies have shown that platinum supported on silica is exceptionally active for naphthalene oxidation [8]. Alongside the investigation of supported metals, there has also been a drive to develop more active metal oxide-based catalysts, as they are cheaper and supplies are more abundant. Previously, we investigated Co_3O_4, Mn_2O_3, ZnO, CuO, Fe_2O_3 and CeO_2, prepared by precipitation, for naphthalene catalytic oxidation [9]. Nanocrystalline CeO_2 with a small crystallite size and high surface area was the most active [10], and it has also been demonstrated that activity could be improved further by the addition of copper to CeO_2 [11]. Mn_2O_3 also showed appreciable activity for naphthalene oxidation, and more in depth studies using high surface area Mn_2O_3, prepared by nanocasting, have identified that it is potentially a catalyst worth further investigation [12]. Against this background, it is interesting to consider the influence of adding copper to manganese oxide for naphthalene oxidation.

Mixed copper manganese oxide (Hopcalite) is well known as an active low-temperature catalyst for the oxidation of carbon monoxide to carbon dioxide [13,14]. Hopcalite has also been studied for the oxidation of a limited range of VOCs including propane [15], toluene [16] and chlorinated VOCs including chlorobenzene [17]. However, to date, mixed copper manganese oxide catalysts have not been studied for the total oxidation of PAHs. In this study, we have, for the first time, investigated the performance of Hopcalite for the total oxidation of the model PAH naphthalene, in order to establish if this inexpensive and readily available catalyst is potentially suitable for control of PAH emissions.

2. Experimental

2.1. Catalyst preparation

Catalysts were prepared using an automated coprecipitation technique. Copper and manganese nitrate solutions (0.25 M) were premixed in a 1:2 ratio. Using a Metrohm titrando autotitrator, the

* Corresponding author. Tel.: +44 029 2087 4062.
E-mail address: taylorsh@cardiff.ac.uk (S.H. Taylor).

http://dx.doi.org/10.1016/j.cattod.2015.01.032
0920-5861/

nitrate solution was mixed with a sodium carbonate solution (2 M) at an appropriate rate to maintain a pH of 8.3 in a stirred precipitation vessel maintained at 80 °C. The resulting precipitate was left to age for 30 min at 80 °C before recovery by filtration, thoroughly washed and then dried for 16 h at 110 °C. Catalysts were generated by calcination of the precursor material in static air for 2 h at 300, 400, 500 and 600 °C. The heating ramp rate was 2 °C min^{-1} starting from ambient temperature

2.2. Catalyst characterisation

Structural phase information on the materials was determined using powder X-Ray diffraction. The data was gathered using a PANalytical X'Pert Pro powder X-ray diffractometer and compared with the ICDD database. The diffractometer was fitted with a Cu source operating at 40 kV and 40 mA.

Thermal gravimetric analysis of the precursor was undertaken using a Setram Labsys TGA/DTA instrument. The sample was heated from 30 to 700 °C under flowing air (15 mL min^{-1}) at a heating rate of 10 °C min^{-1}. The mass change and the heat flow of the sample was monitored.

Temperature-programmed reduction (TPR) analysis of the catalysts was performed using a Quantachrome ChemBET TPD/R/O apparatus. In total, 30 mg sample of each catalyst was heated to 600 °C at a rate of 15 °C min^{-1} under a flow of 10%H_2/Ar at a flow rate of 30 mL min^{-1}.

The surface area of the catalysts was determined using the BET method. The catalysts were degassed by flushing with dry N_2 for 0.5 h at a temperature of 120 °C to avoid catalysts becoming nonstoichiometric by degassing under vacuum. A 5-point N_2 adsorption isotherm was measured at −196 °C using a Micromeritics Gemini 2360 instrument.

2.3. Catalytic activity determination

Catalyst activity was determined using a standard fixed-bed gas flow microreactor. A 100 vppm flow of naphthalene was generated by heating naphthalene (scintillation grade, Sigma–Aldrich) in a tube furnace under a flow of helium. Oxygen was then added to give a total flow of 40 mL min^{-1} (20% O_2 balance He). This was flowed through a fixed bed of the catalyst, which was packed to a constant volume to give a gas hourly space velocity of 60,000 h^{-1}. The catalyst temperature was controlled by a thermocouple placed in the catalyst bed, and activity was measured over the temperature range 150–350 °C using incremental temperature steps. At each temperature, the catalyst was allowed to stabilise and steady-state activity was measured. The gaseous effluent was measured using an on-line Varian 3400 gas chromatograph fitted with OV-17 and Carbosive columns with flame ionisation and thermal conductivity detectors.

In order to analyse the stability of the catalysts on-stream, a sample was tested at a constant temperature of 350 °C and products analysed every hour for 48 h. To investigate the reusability of the catalyst, a sample was tested for three successive cycles, raising the catalyst temperature to a maximum of 350 °C for each cycle, before cooling and restarting the cycle.

3. Results and discussion

3.1. Catalyst and precursor characterisation

Fig. 1a shows the X-ray diffraction pattern of the catalyst precursor (material obtained after drying the precipitate before calcination). The only phase observed was that of the hexagonal-rhombohedra $MnCO_3$ phase. This was indicated by the principle reflection at 32° corresponding to the (114) set of lattice planes. The reflection associated with the (012) plane was also clearly observed at 24.5°, as was the (116) at 52.2°. No evidence was observed for reflections that corresponded to a copper-containing phase. However, when compared with a standard $MnCO_3$ diffraction pattern, the peaks appear shifted to higher 2θ angles by around 0.5°. In the standard $MnCO_3$ sample, the (114) plane is observed at 31.4°, the (012) plane at 24.3° and the (116) plane at 51.7. This is consistent with previous work by Porta et al., who demonstrated that when copper is substituted into the $MnCO_3$ lattice, the unit cell contracts due to the smaller ionic radius of copper, site distortion due to the d^9 electron configuration as well as the higher covalency of the copper–oxygen polyhedral [18]. Indeed, previous work on related copper manganese oxide catalysts prepared mechanochemically

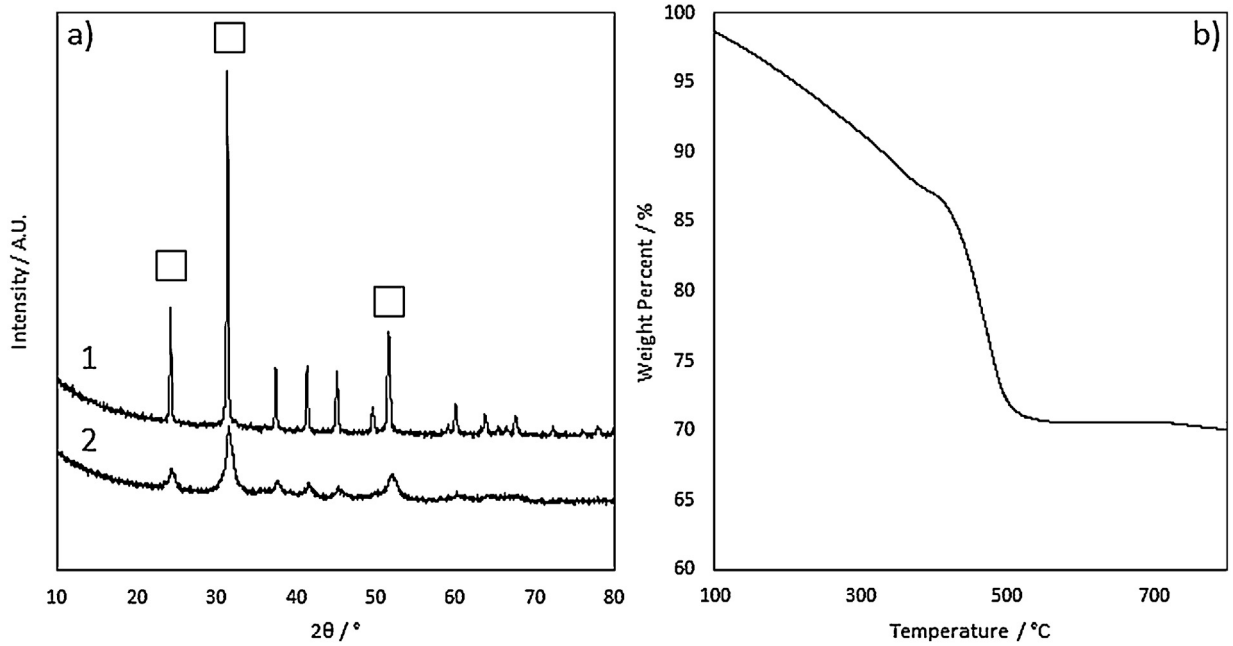

Fig. 1. a. Powder X-ray diffraction patterns of precursor materials 1. Standard $MnCO_3$, 2. Copper manganese oxide catalyst precursor. □ = $MnCO_3$. b. Thermal gravimetric analysis profile of the catalyst precursor.

Please cite this article in press as: T.J. Clarke, et al., Total oxidation of naphthalene using copper manganese oxide catalysts, Catal. Today (2015), http://dx.doi.org/10.1016/j.cattod.2015.01.032

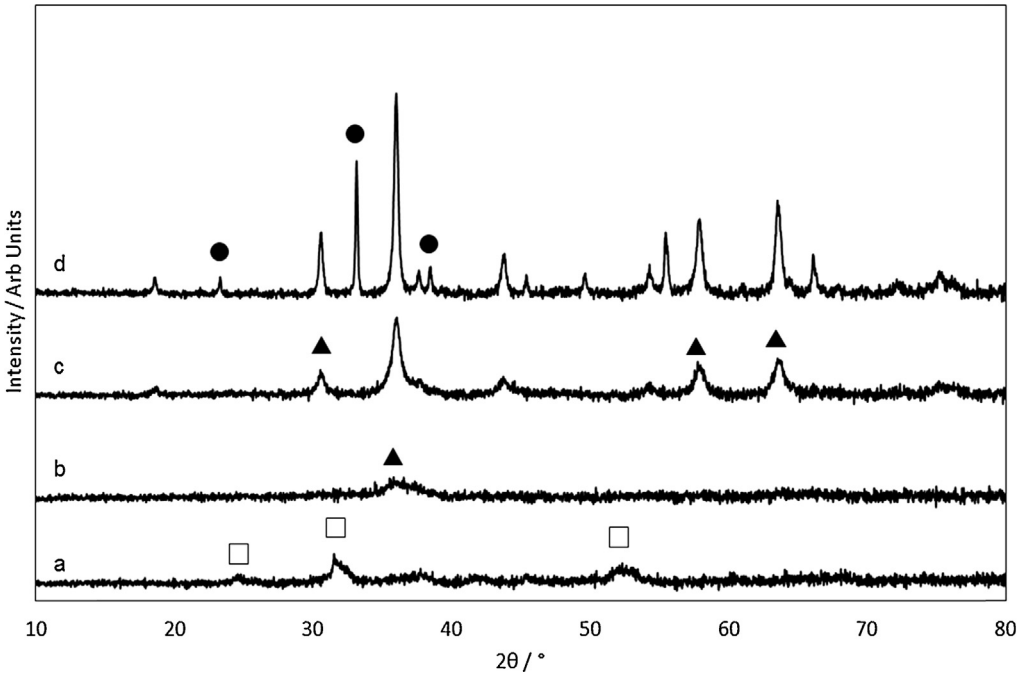

Fig. 2. Powder X-ray diffraction patterns of calcined copper manganese oxide catalysts a. 300 °C, b. 400 °C, c. 500 °C, and d. 600 °C. □ = $MnCO_3$, ● = Mn_2O_3, ▲ = $CuMn_2O_4$.

showed a decrease in the lattice parameter of $MnCO_3$, as increased concentrations of Cu^{2+} were incorporated [19].

The TGA profile of the catalyst precursor (Fig. 1b) showed two weight-loss events. The first broad mass loss from 100 to 350 °C is associated with the loss of physisorbed and chemisorbed water from the precursor material and makes up 13% of the total mass. The second loss at 400 °C was due to the decomposition of $MnCO_3$ with associated evolution of CO_2. This second mass loss was *ca.* 20% of the total mass. If the precursor material was $MnCO_3$ alone, the theoretical mass loss would be *ca.* 30%. Possibly, suggesting that $MnCO_3$ was not the only phase present. The absence of diffraction from another phase indicates that it is either amorphous, or at least present as very small crystallites. This interpretation is somewhat speculative and the discrepancy could be equally explained by a change of the carbonate stoichiometry, possibly by substitution of Cu ions into the Mn lattice. Further characterisation studies would be required to provide a definitive explanation.

X-ray diffraction patterns of the calcined catalysts investigated for naphthalene oxidation are shown in Fig. 2. The catalyst calcined at 300 °C still consisted of $MnCO_3$ with no evidence for formation of the spinel $CuMn_2O_4$ phase. This is, maybe, not unexpected, as the TGA profile in Fig. 1b shows that significant decomposition of $MnCO_3$ did not begin until 400 °C.

After calcination at 400 °C the reflections that correspond to $MnCO_3$ were no longer visible. There was only one observable diffraction peak, which was a very broad feature at 36.1°. This could correspond with the (311) lattice plane of $CuMn_2O_4$; however, as there are no other visible reflections, it is difficult to be certain, as the (311) reflection is the most intense, it is unsurprising that no others are visible, given how weak it is. The absence of other reflections and the broad nature of the peak suggest a nanocrystalline or highly disordered material.

The precursor calcined at 500 °C showed clear evidence for formation of the spinel $CuMn_2O_4$ phase. The peak at 36.3° can be assigned to diffraction of the (311) planes and the reflections at 57.5 and 63.1° can be attributed to the diffraction from the (511) and (440) planes, respectively.

Calcination at 600 °C resulted in a mixture of phases, with evidence of a Mn_2O_3 phase present with a mixed copper manganese oxide phase. The reflection observed at 33.1° is characteristic of the (222) lattice planes of Mn_2O_3. The reflections associated with $CuMn_2O_4$ are now more easily observed, and they are narrower and more intense than those after calcination at lower temperatures, suggesting that the mixed copper manganese oxide phase has longer-range crystallinity after calcination at higher temperature.

The BET surface areas for the catalysts prepared at different calcination temperatures are shown in Table 1. The sample calcined at

Table 1
Physical properties of the tested catalysts.

Calcination temperature/°C	Surface area/$m^2\ g^{-1}$	Phases present	H_2 consumed/mmol g^{-1}	T_{50}[a]/°C	T_{90}[a]/°C	T for 50% naphthalene coversion/°C	T for 90% naphthalene coversion/°C	CO_2 selectivity at 50% conversion/%
Uncalcined	5	$MnCO_3$	–	–	–	–	–	–
300	9	$MnCO_3$	7.4	242	250	242	250	100
400	72	$CuMn_2O_4$	12.4	229	238	228	238	99
500	52	$CuMn_2O_4$	8.7	239	270	230	258	30
600	14	$CuMn_2O_4$, Mn_2O_3	7.2	269	290	248	262	20
Comparison catalysts								
1% Pt/Al_2O_3	–	–		250	280	–		–
Commercial Hopcalite	–	–		226	245	226	245	100

[a] Temperature for 50 and 90% conversion to CO_2

Please cite this article in press as: T.J. Clarke, et al., Total oxidation of naphthalene using copper manganese oxide catalysts, Catal. Today (2015), http://dx.doi.org/10.1016/j.cattod.2015.01.032

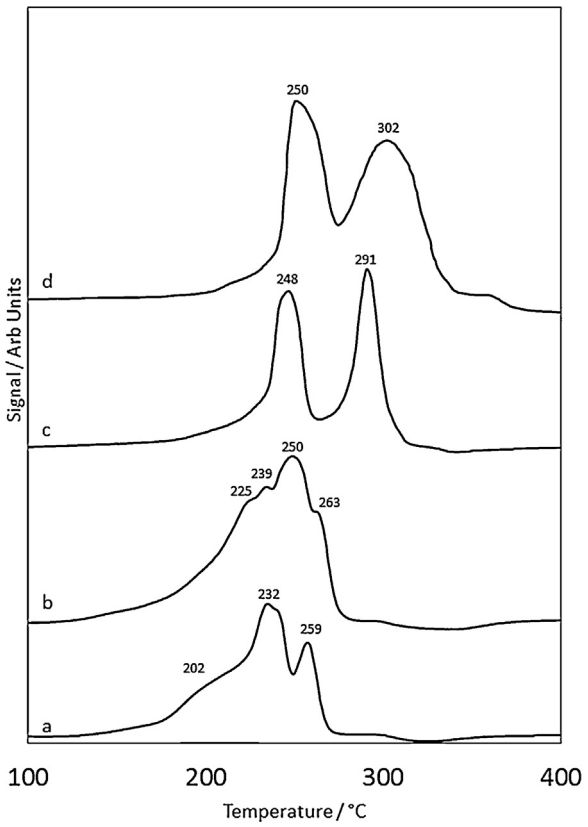

Fig. 3. Hydrogen temperature-programmed reduction profiles of catalyst materials a. 300 °C, b. 400 °C, c. 500 °C, and d. 600 °C.

300 °C showed a very low surface area, characteristic of manganese carbonate. At 400 °C, the surface area is dramatically increased to 72 $m^2 g^{-1}$, and this is related to formation of a nanocrystalline $CuMn_2O_4$ phase [14]. As the calcination temperature increased further, the catalyst surface area decreased, as would be expected due to the effects of sintering of crystallites of the mixed copper manganese oxide phase. At the highest calcination temperature, the formation of the low surface area Mn_2O_3 phase further depresses the overall surface area of the material [12].

Temperature-programmed reduction (TPR) of the materials is shown in Fig. 3. The results showed a complex series of overlapping peaks, which are often observed for copper manganese oxides. After calcination at 300 °C, the catalyst showed a broad peak centred at 202 °C followed by sharper peaks at 232 and 259 °C. These peaks are attributed to the complex reduction of the copper-substituted manganese carbonate phase. When calcined at 400 °C, there were multiple peaks with the main peak at 250 °C. This is attributed to the reduction of the nanocrystaline $CuMn_2O_4$ phase with the other shoulders possibly arising from residual carbonate reduction. At 500 °C, the profile is that of a typical crystalline spinel $CuMn_2O_4$ reduction with a two stage reduction at 248 and 291 °C [20]. In their study of copper manganese oxide, Buciuman et al. attribute the two-step reduction to the reduction of the two different cations present in the spinel structure with the Cu^{2+} component reducing initially to Cu^0 followed by the reduction of the Mn^{3+} to the Mn $^{2+}$species [20]. After 600 °C calcination, the highest studied, the two-step reduction profile remained; however, the higher temperature peak is broadened due to the contribution from the reduction of the Mn_2O_3 phase to MnO. The extent of reducibility of the catalysts was determined by measuring the total hydrogen consumption during the reduction (Table 1). The catalyst calcined at 400 °C contained the greatest amount of reducible material, and hence, has the largest concentration of labile oxygen. For calcination at 300 °C, the material was less reducible, presumably due to the incomplete formation of the oxide phases. As calcination temperatures were increased, the total amount of reducible material decreased, this is attributed to the higher crystallinity of these materials and the resulting decrease in lattice oxygen mobility.

3.2. Catalytic activity

Figure 4a shows the formation of CO_2 as a function of catalyst temperature, and comparisons with a commercially available Hopcalite and a commercial 1% Pt/Al_2O_3 catalyst have been made. From data in Fig. 4a and T_{50} and T_{90} measurements for CO_2 formation (Table 1), the catalyst calcined at 400 °C was the most active. This can be related to the presence of the amorphous $CuMn_2O_4$ phase that has previously been shown to be important for CO oxidation [13] and propane total oxidation [15]. This maximum of activity correlates with the TPR data (Table 1), that showed that the catalyst calcined at 400 °C had the highest extent of reduction and the highest amount of labile oxygen species. The catalyst calcined at 300 °C showed lower activity, and this can be related to the presence of $MnCO_3$, which was not converted to the oxide during calcination. Calcination at higher temperatures increased the temperature required for naphthalene total oxidation. This can be observed by considering the T_{50} and T_{90} values, *i.e.* the temperatures required to achieve 50 and 90% naphthalene conversion to CO_2, respectively. For example, T_{50} for the catalyst calcined at 500 °C was 10 °C higher and the material calcined at 600 °C had a T_{50} 40 °C higher than the material calcined at 400 °C.

The catalytic activity was also analysed in terms of naphthalene conversion (Fig. 4b). The trend of the data is the same with 400 °C being the most active for naphthalene conversion. The T_{50} values for the 400 °C calcined catalyst were similar when CO_2 yield and naphthalene conversion were compared. Furthermore, the T_{50} values for naphthalene conversion for the 400 and 500 °C catalysts were similar. However, for both the catalysts calcined at 500 and 600 °C, the temperature for 50% naphthalene conversion was obtained at a lower temperature than the T_{50} for CO_2 formation (Table 1). These differences between naphthalene conversion and CO_2 yield indicate that the catalysts calcined at 500 and 600 °C are less selective towards CO_2 than the catalyst calcined at 400 °C. These discrepancies between CO_2 formation and naphthalene conversion suggest the formation of naphthalene partial oxidation products. Previous work on naphthalene oxidation from our group has shown that partial oxidation products are commonly produced, and we found that benzoic acid and phthalic anhydride were common by-products [9]. Based on our experience, we consider that similar products are also produced in the study with selected catalysts, but at this preliminary stage, we have not specifically analysed for them. It is also possible that partial oxidation products are formed as primary products over the most active catalyst calcined at 400 °C, however, they are rapidly oxidised to CO_2 before exiting the catalyst bed. The catalytic data suggests that poorly crystalline $CuMn_2O_4$ is the most active phase for the total oxidation of naphthalene, with more highly crystalline $CuMn_2O_4$ and less active Mn_2O_3 phases. The more crystaline $CuMn_2O_4$ phase also appears to have poorer selectivity towards CO_2 than the more disordered phase, as seen in the material calcined at 500 °C. Partial oxidation of naphthalene has been observed in previous work by Garcia et al. when using manganese oxide catalysts, this phase could be responsible for the low-CO2 selectivity for the catalyst calcined at 600 °C, as Mn_2O_3 was a major catalyst component [9]. The formation of partial oxidation products could also be directly related to the surface area of the catalysts, as the catalyst calcined at 400 °C (negligible partial oxidation products) has a greater surface area to re-adsorb and

Please cite this article in press as: T.J. Clarke, et al., Total oxidation of naphthalene using copper manganese oxide catalysts, Catal. Today (2015), http://dx.doi.org/10.1016/j.cattod.2015.01.032

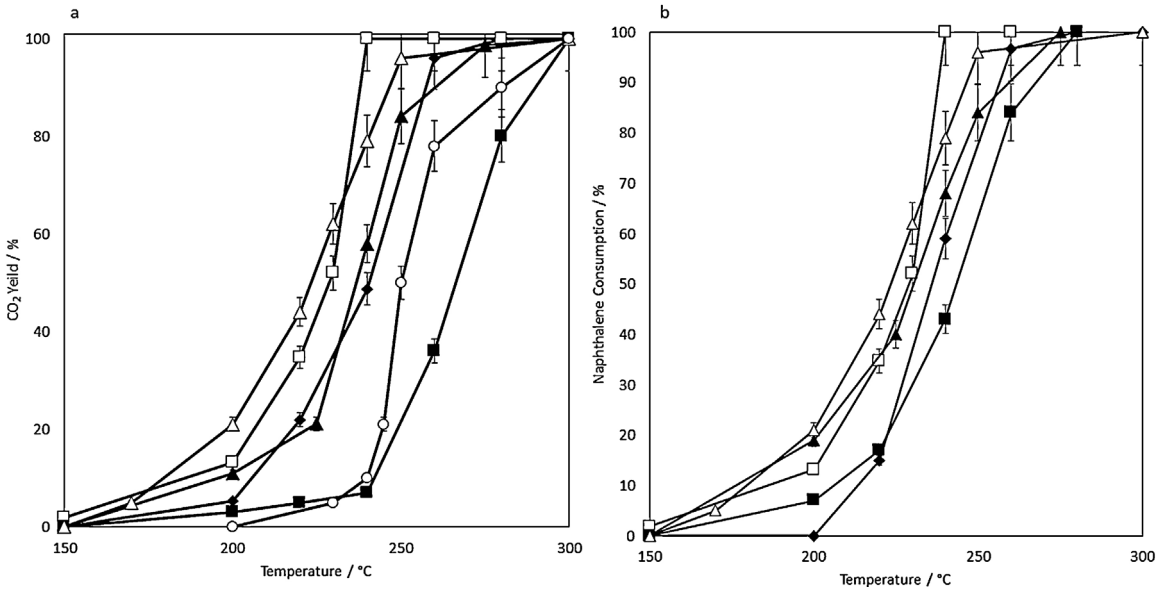

Fig. 4. a. Light-off curve for CO_2 production from catalytic naphthalene oxidation, b. Light-off curve for naphthalene conversion over the range of catalysts. ♦ = 300 °C, □ = 400 °C, ▲ = 500 °C, ■ = 600 °C, △ = Commercial Hopcalite, ○ = 1% Pt/Al_2O_3. Error = ± 6.7%.

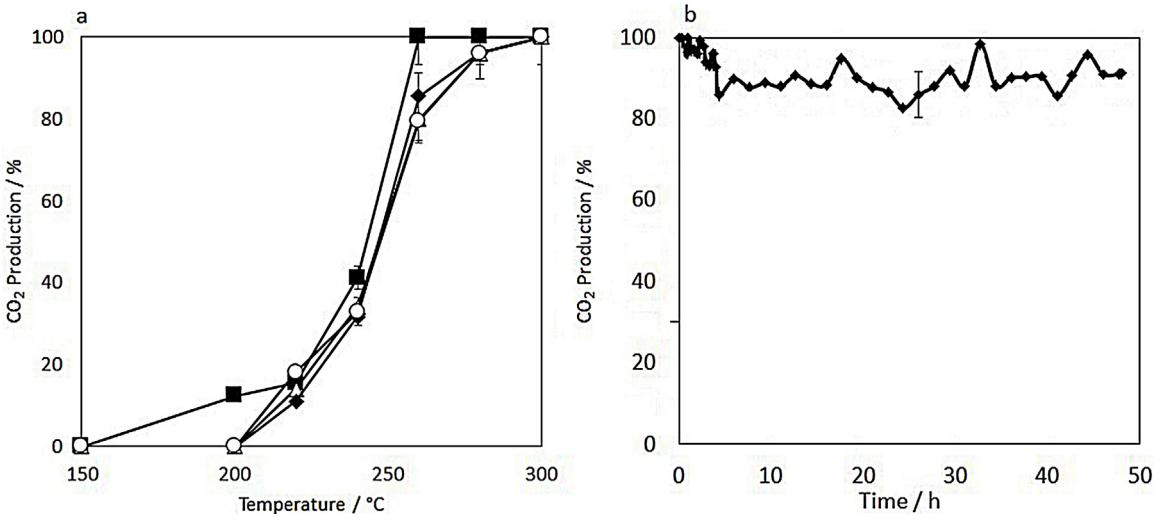

Fig. 5. a. Conversion of naphthalene to CO2 in successive reaction cycles using the catalyst calcined at 400 °C, ■ = Cycle 1, △ = Cycle 2, ♦ = Cycle 3, ○ = Cycle 4. Error = ± 6.7%; b. *Time-on-stream* catalyst stability test of material calcined at 400 °C. Error = ± 6.7%.

further oxidise partially oxidised products when compared with the catalysts calcined at higher temperatures.

It is interesting to benchmark the performance of the coprecipitated copper manganese oxide catalysts, as there are no previous data available for naphthalene oxidation (Table 1). When compared with a commercially available copper manganese oxide catalyst, the coprecipitated catalyst calcined at 400 °C performed similarly with comparable T_{50} and T_{90} values. However, the composition of the commercial catalyst is more complex than copper manganese oxide alone and also contains promoter materials that are not present in the coprecipitated catalysts prepared in this study. Commonly, supported noble metal catalysts have been successfully used for naphthalene total oxidation. Comparison with a commercial 1% Pt/Al_2O_3 catalyst demonstrated that the coprecipitated copper manganese oxide catalysts were more active when compared in terms of T_{50} and T_{90}.

The stability of the most active catalyst, prepared by calcination at 400 °C, was evaluated by cycling through a series of light-off experiments and by measuring activity as a function of *time-on-stream*. The results of temperature cycling experiments are shown in Fig. 5a. After the first *light-off* curve, there was a slight deactivation of the catalyst. Subsequent light-off curves were superimposable with each other, indicating that after the initial use, there was no further catalyst deactivation. The catalyst was also subjected to an accelerated ageing *time-on-stream* experiment for 48 h at 350 °C. As shown in Fig. 5b, the activity of the catalyst decreased from 100 to around 90% within the first 4 h of testing. The activity then stabilised at this level for the remainder of the experiment and there was no further evidence of catalyst deactivation. The deactivation observed could be due to several factors, such as loss of surface area or increased surface concentration of species like CO_2 or partially oxidised products. Further studies would be required to confirm the definitive reason.

4. Conclusions

Precipitated copper manganese oxide catalysts are active for naphthalene total oxidation. A poorly crystalline $CuMn_2O_4$ phase

Please cite this article in press as: T.J. Clarke, et al., Total oxidation of naphthalene using copper manganese oxide catalysts, Catal. Today (2015), http://dx.doi.org/10.1016/j.cattod.2015.01.032

was more active than the crystalline spinel phase. The optimum calcination temperature for these catalysts was 400 °C. Lower calcination temperatures were insufficient to generate the active $CuMn_2O_4$ phase. At higher calcination temperatures, the increased crystallinity of the catalysts and lower surface areas resulted in lower total oxidation activity, also demonstrated by the production of more undesirable partially oxidised products. A direct relationship between the performance for naphthalene oxidation and the extent of reduction of the catalyst was observed, indicating that the lability of oxygen species of the catalyst are important. The most active catalyst, prepared after calcination at 400 °C, demonstrated higher activity for naphthalene oxidation than a supported platinum catalyst, and was at least equivalent to a commercial Hopcalite catalyst. Furthermore, the catalyst was stable on reuse, showing a slight deactivation after the first use, but no further deactivation thereafter. Slight deactivation was also observed with prolonged *time-on-stream*, but this was only in the first 4 h and then stable high activity was maintained.

References

[1] S.H. Taylor, B. Solsona, T. Garcia, The catalytic oxidation of hydrocarbon Volatile Organic Compounds, in: F.C.D. Duprez (Ed.), Advanced Processes in Catalytic Oxidation. From Laboratory Studies to Industrial Applications, Imperial College Press, London, UK, 2014, pp. 51–90.
[2] J.J. Levy, E.A. Houseman, J.D. Spengler, P. Loh, L. Ryan, Fine particulate matter and polycyclic aromatic hydrocarbon concentration patterns in Roxbury, Massachusetts: a community-based GIS analysis, Environ. Health Persp. 109 (2001) 341–347.
[3] E. Union, PAH Position Paper ISBN92-894-2057-X, Office for Official Publications of the European Communities, Luxembourg, 2001.
[4] N.E. Ntainjua, S. Taylor, The catalytic total oxidation of polycyclic aromatic hydrocarbons, Top. Catal. 52 (2009) 528–541.
[5] X.-W. Zhang, S.-C. Shen, L.E. Yu, S. Kawi, K. Hidajat, K.Y. Simon Ng, Oxidative decomposition of naphthalene by supported metal catalysts, Appl. Catal. A: Gen. 250 (2003) 341–352.
[6] J.-L. Shie, C.-Y. Chang, J.-H. Chen, W.-T. Tsai, Y.-H. Chen, C.-S. Chiou, C.-F. Chang, Catalytic oxidation of naphthalene using a Pt/Al_2O_3 catalyst, Appl. Catal. B: Environ. 58 (2005) 289–297.
[7] F. Klingstedt, A. Kalantar Neyestanaki, L.E. Lindfors, T. Salmi, T. Heikkilä, E. Laine, An investigation of the activity and stability of Pd and Pd-Zr modified Y-zeolite catalysts for the removal of PAH, CO, CH_4 and NO_x emissions, Appl. Catal. A: Gen. 239 (2003) 229–240.
[8] N.E. Ntainjua, A.F. Carley, S.H. Taylor, The role of support on the performance of platinum-based catalysts for the total oxidation of polycyclic aromatic hydrocarbons, Catal. Today 137 (2008) 362–366.
[9] T. García, B. Solsona, S.H. Taylor, Naphthalene total oxidation over metal oxide catalysts, Appl. Catal. B: Environ. 66 (2006) 92–99.
[10] T. Garcia, B. Solsona, S. Taylor, Nano-crystalline ceria catalysts for the abatement of polycyclic aromatic hydrocarbons, Catal. Lett. 105 (2005) 183–189.
[11] A. Aranda, E. Aylon, B. Solsona, R. Murillo, A.M. Mastral, D.R. Sellick, S. Agouram, T. Garcia, S.H. Taylor, High activity mesoporous copper doped cerium oxide catalysts for the total oxidation of polyaromatic hydrocarbon pollutants, Chem. Commun. 48 (2012) 4704–4706.
[12] T. Garcia, D. Sellick, F. Varela, I. Vázquez, A. Dejoz, S. Agouram, S.H. Taylor, B. Solsona, Total oxidation of naphthalene using bulk manganese oxide catalysts, Appl. Catal. A: Gen. 450 (2013) 169–177.
[13] G.J. Hutchings, A.A. Mirzaei, R.W. Joyner, M.R.H. Siddiqui, S.H. Taylor, Ambient temperature CO oxidation using copper manganese oxide catalysts prepared by coprecipitation: effect of ageing on catalyst performance, Catal. Lett. 42 (1996) 21–24.
[14] C. Jones, K.J. Cole, S.H. Taylor, M.J. Crudace, G.J. Hutchings, Copper manganese oxide catalysts for ambient temperature carbon monoxide oxidation: effect of calcination on activity, J. Mol. Catal. A: Chem. 305 (2009) 121–124.
[15] B. Solsona, T. Garcia, S. Agouram, G.J. Hutchings, S.H. Taylor, The effect of gold addition on the catalytic performance of copper manganese oxide catalysts for the total oxidation of propane, Appl. Catal. B: Environ. 101 (2011) 388–396.
[16] H.C. Genuino, S. Dharmarathna, E.C. Njagi, M.C. Mei, S.L. Suib, Gas-phase total oxidation of benzene, toluene, ethylbenzene, and xylenes using shape-selective manganese oxide and copper manganese oxide catalysts, J. Phys. Chem. C 116 (2012) 12066–12078.
[17] V.H. Vu, J. Belkouch, A. Ould-Dris, B. Taouk, Removal of hazardous chlorinated VOCs over Mn–Cu mixed oxide based catalyst, J. Hazard. Mater. 169 (2009) 758–765.
[18] P. Porta, G. Moretti, M.L. Jacono, M. Musicanti, A. Nardella, Characterization of copper-manganese hydroxysalts and oxysalts, J. Mater. Chem. 1 (1991) 129–135.
[19] T.J. Clarke, T.E. Davies, S.A. Kondrat, S.H. Taylor, Mechanochemical synthesis of copper manganese oxide for the ambient temperature oxidation of carbon monoxide, Appl. Catal. B: Environ. 165 (2015) 222–231.
[20] F.C. Buciuman, F. Patcas, T. Hahn, A spillover approach to oxidation catalysis over copper and manganese mixed oxides, Chem. Eng. Process. 38 (1999) 563–569.

Please cite this article in press as: T.J. Clarke, et al., Total oxidation of naphthalene using copper manganese oxide catalysts, Catal. Today (2015), http://dx.doi.org/10.1016/j.cattod.2015.01.032